Expression of expanded *FMR1*-CGG repeats alters mitochondrial miRNAs and modulates mitochondrial functions and cell death in cellular model of FXTAS

Dhruv Gohel [a], Lakshmi Sripada [a], Paresh Prajapati [b], Fatema Currim [a], Milton Roy [a], Kritarth Singh [c], Anjali Shinde [a], Minal Mane [a], Darshan Kotadia [a], Flora Tassone [d], Nicolas Charlet-Berguerand [e], Rajesh Singh [a,*]

[a] *Department of Biochemistry, Faculty of Science, The M.S. University of Baroda, Vadodara, 390002, Gujarat, India*
[b] *SCoBIRC Department of Neuroscience, University of Kentucky, 741S. Limestone, BBSRB, Lexington, KY, 40536, USA*
[c] *Department of Cell and Developmental Biology, University College London, Gower Street, London, WC1E 6BT, UK*
[d] *Medical Investigation of Neurodevelopmental Disorders (MIND) Institute, University of California Davis, Davis, CA, 95817, USA*
[e] *Institut de Genetique et de Biologie Moleculaire et Cellulaire (IGBMC), INSERM U1258, CNRS UMR7104, Universit´e of Strasbourg, 67400, Illkirch, France*

ARTICLE INFO

Keywords:
FXTAS
Mito-miRs
miR-320a
Mitotranscripts
Ago2
OXPHOS
Mitochondrial dysfunctions
Cell death

ABSTRACT

Fragile X-associated tremor/ataxia syndrome (FXTAS) is a progressive neurodegenerative disorder caused by an expansion of 55 to 200 CGG repeats located within 5′UTR of *FMR1*.These CGG repeats are transcribed into RNAs, which sequester several RNA binding proteins and alter the processing of miRNAs. CGG repeats are also translated into a toxic polyglycine-containing protein, FMRpolyG, that affects mitochondrial and nuclear functions reported in cell and animal models and patient studies. Nuclear-encoded small non-coding RNAs, including miRNAs, are transported to mitochondria; however, the role of mitochondrial miRNAs in FXTAS pathogenesis is not understood. Here, we analyzed mitochondrial miRNAs from HEK293 cells expressing expanded CGG repeats and their implication in the regulation of mitochondrial functions. The analysis of next generation sequencing (NGS) data of small RNAs from HEK293 cells expressing CGG premutation showed decreased level of cellular miRNAs and an altered pattern of association of miRNAs with mitochondria (mito-miRs). Among such mito-miRs, miR-320a was highly enriched in mitoplast and RNA immunoprecipitation of Ago2 (Argonaute-2) followed by Droplet digital PCR (ddPCR)suggested that miR-320a may form a complex with Ago2 and mitotranscripts. Finally, transfection of miR-320a mimic in cells expressing CGG permutation recovers mitochondrial functions and rescues cell death. Overall, this work reveals an altered translocation of miRNAs to mitochondria and the role of miR-320a in FXTAS pathology.

1. Introduction

FXTAS is a late onset inherited neurodegenerative disorder characterized by progressive intention tremor, gait ataxia and cognitive decline [1,2]. Nearly,1 in ~3000 male and 1 in ~5000 female can be affected by FXTAS and disease symptoms get more pronounced with the age [3]. FXTAS is caused by an expansion of 55 to 200 CGG repeats (known as premutation) at the 5′UTR of the *FMR1* gene located on the long arm of X chromosome [4]. The expanded CGG repeats are transcribed into RNAs that titrate specific RNA binding proteins such as the DROSHA/DGCR8 complex involved in regulation of the processing of microRNAs (miRNAs) [5]. Consequently, expression of various miRNAs are altered in FXTAS [6,7]. CGG repeats embedded in the 5′UTR of *FMR1* are translated into a toxic polyglycine-containing protein, FMRpolyG, through initiation via a non-canonical ACG start codon located upstream of the repeats [8–10]. However, it is still not understood if CGG RNA and/or FMRpolyG protein contribute to mitochondrial alterations leading neuronal cell dysfunctions and death [11].Importantly, recent findings suggest that mitochondrial dysfunctions including loss of mitochondrial membrane potential, ATP and mitochondrial transcripts and proteins are associated with FXTAS pathogenesis [11–14]. We have recently shown decreased expression levels of mitochondrial transcripts

* Corresponding author.
E-mail address: rajesh.singh-biochem@msubaroda.ac.in (R. Singh).

in FXTAS leading to altered mitochondrial supercomplexes assembly and individual complex activity in cellular models and transgenic mice expressing expanded CGG repeats [15].However, the molecular mechanisms regulating mitochondrial dysfunction in FXTAS conditions are not well understood.

miRNAs belong to a class of noncoding RNAs important for post transcriptional regulation of mRNAs by partial base-pairing of miRNA-mRNA mediated by the RNA-induced silencing complexes (RISC) [16, 17]. Studies from last decade have shown evidences of organelle specific localization of miRNAs and presence of crucial RISC component like Ago2 in the mitochondria [18,19]. We and others have also reported that specific nuclear encoded miRNAs translocate to mitochondria (referred as mito-miRs) under specific stimuli and can regulate mitochondrial functions [20,21]. As miRNAs expression and mitochondrial functions are altered in FXTAS, we investigated mito-miRs and their potential role in mitochondrial bioenergetics in FXTAS *in vitro* cellular model. Interestingly, we identified a specific population of miRNAs which was altered in mitochondrial fractions in cells expressing expanded CGG repeats. Among these miRNAs, we analyzed the role of miR-320a, which was specifically enriched in mitochondria in FXTAS condition. Finally, transfection of miR-320a mimic showed increased OXPHOS activity, suggesting a crucial role of miR-320a in FXTAS pathology.

2. Material and methods

2.1. Cell culture

HEK293 cells were grown in Dulbecco's Modified Eagle's Medium (DMEM, Gibco, Invitrogen, USA), SH-SY5Y cells were grown in DMEM-F12 (Gibco, Invitrogen, USA), and U87MG cells were grown in MEM (Minimal Essential Medium, Gibco, Invitrogen, USA) supplemented with 10% (v/v) heat-inactivated fetal bovine serum (Gibco, Invitrogen, USA), 1% penicillin, streptomycin and neomycin (PSN) antibiotic mixture (Gibco, Invitrogen, USA). The cells were maintained in5% CO_2 at 37 ◦C.

2.2. Construct details

Mainly two CGG repeats constructs: ATG FMRpolyG-GFP and 5′UTR *FMR1* CGG99X (fused with GFP) were used for transfection for

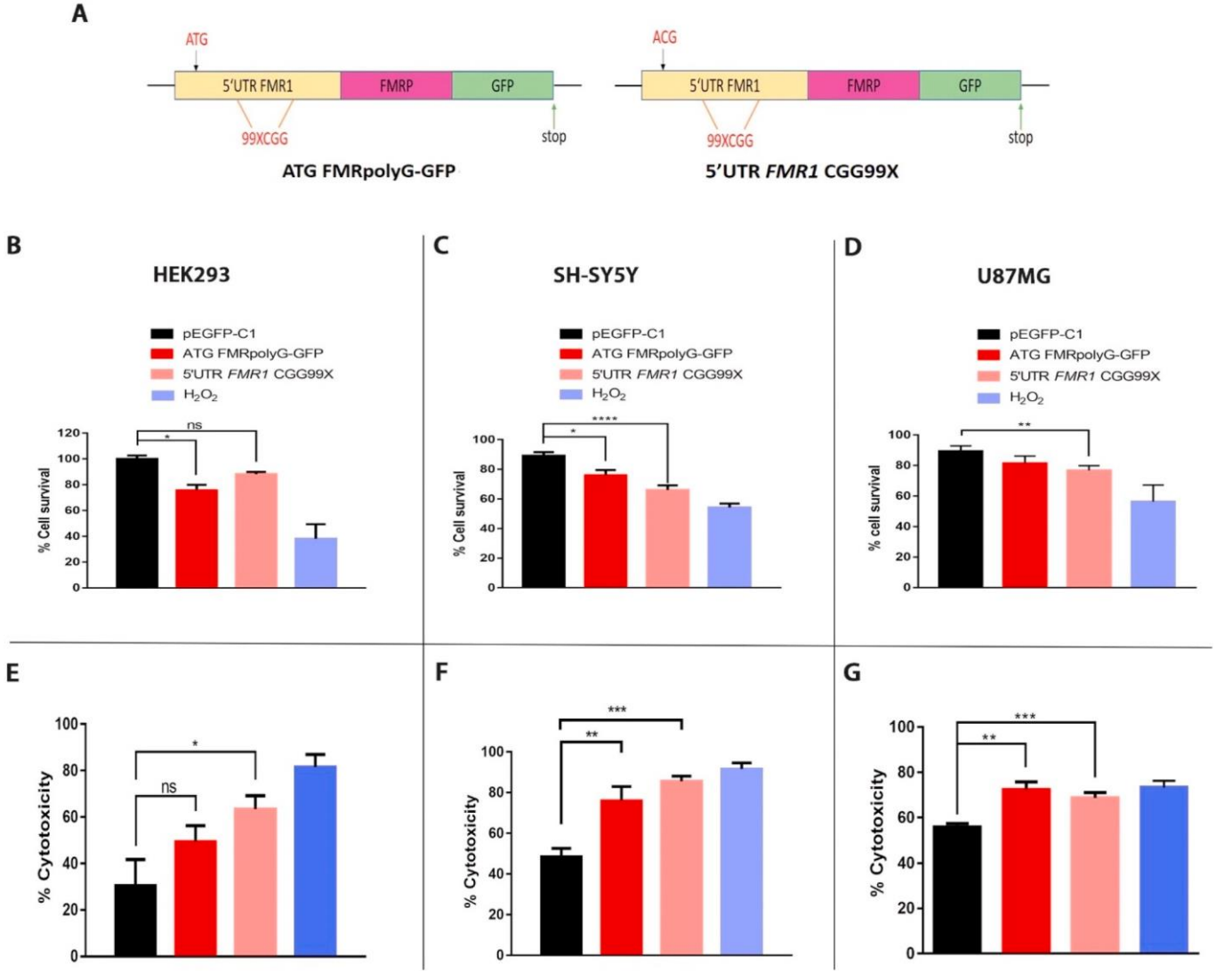

Fig. 1. Expression of expanded CGG repeats causes decreased cell survival increased apoptosis. Schematic representation of constructs (ATG FMRpolyG-GFP and 5′UTR*FMR1* CGG99X) used for mimicking *in vitro*FMR1 premutation condition. (A) Both the constructs expressing CGG repeats were transfected and cellular viability was determined by XTT assay in HEK293 (B), and SH-SY5Y(C) and U87MG (D) cells. FMRpolyG induced cytotoxicity in HEK293 (E), SH-SY5Y (F), and U87MG (G) cells was measured by staining the cells with Propidium Iodide (PI) (n = 3) $p > 0.05$ (ns), $p \leq 0.05$ (*),$p \leq 0.01$ (**), $p \leq 0.001$ (***).

mimicking FXTAS condition *in vitro* (Fig. 1A). ATG FMRpolyG-GFP, which has canonical start codon (ATG) before the expanded CGG repeats constitutively expresses FMRpolyG while 5′UTR *FMR1* CGG99X contain non canonical codon (ACG) before the CGG repeats leads to formation of FMRpolyG mainly due to RAN translation, more resembles premutation condition. pEGFP-C1 was used as control for all the experiments.

2.3. Transfection of mimic

The control RNA (scrambled sequence) and mimic of miR-320a (mirVana, Thermofisher, USA) were transfected using Lipofectamine RNAiMAX(Thermofisher, USA)following manufacturer's instructions. Briefly, the miRNA mimic and control (final concentration of 30 nM) and Lipofectamine RNAiMAX reagent was diluted in OptiMEM (Life Technologies, USA). The miRNA mix was added to Lipofectamine mix and incubated for 15 min and added to the cells. The media was replaced after 10 h and further incubated/treated as per requirement in different assays.

2.4. Kits and reagents

Primers for all miRNAs, actin, 5S RNA, U6 snRNA and mitotranscripts were purchased from IDT, USA (Primer detail: Supplementary Table S1). XTT (2,3-Bis-(2-Methoxy-4-Nitro-5-Sulfophenyl)-2H-Tetrazolium-5-Carboxanilide), MTT (3-(4,5-Dimethylthiazol-2-yl)-2,5-Diphenyltetrazolium Bromide) andCM-H2DCFDA was purchased from Thermofisher, USA. Antibodies used for all immunoblotting were purchased from Cell Signaling Technology (CST), USA. RNase A and buffer P1 were used from QIAprep Spin Miniprep Kit (Qiagen, Netherlands). SYBR green and cDNA isolation kits were purchased from Takara, Japan. MicroAmp Fast Optical 96-Well Reaction Plate, MicroAmp Optical Adhesive Film, Lipofectamine 2000, Opti-MEM was procured from Thermofisher, USA.

2.5. Cell viability and cell death assays

HEK293, SH-SY5Y and U87MG cells were plated at density of 5×10^3 cells/well in 96 well plate and transfected with indicated constructs. After 24 h of transfection, XTT assay was performed to check altered mitochondrial metabolism as per the manufacturer's instructions with minor modifications. The cellular viability was further determined by MTT assay as described previously [22]. Briefly, $5X10^3$ cells were plated in 96 well plate and transfected with 5′UTR *FMR1* CGG99X along with control and mimic of miR-320a as described above. After 24 h of transfection, MTT was performed by incubating cells with 0.1 mg/ml MTT for 2 h at 37 °C. The formazan crystals were then dissolved in DMSO and absorbance was measured at 570 nm using microplate reader Synergy HTX (Biotech Instruments, USA). Percentage cells undergoing apoptosis were determined by staining the cells with 10 μM Propidium Iodide (#P1304MP, Thermofisher, USA) solution for 30 min followed by washing with 1X DPBS. Fluorescence intensity was measured at 617 nm. The resultant fluorescence was normalized to calculate percentage cell death.

Western blotting was performed to check expression levels of several death makers including PARP cleavage and active caspases. Briefly, cell HEK293 cells were seeded at a density of 4.5×10^5 per well in six well plate and miR-320a was co transfected along with CGG repeats constructs. After 24 h of transfection, cells were harvested, washed with ice cold PBS and lysed in NP40 lysis buffer (150 mM NaCl, 50 mM Tris–Cl, 1% NP40, 1 mM PMSF). Protein concentration was determined by Bradford assay and equal protein resolved on 10% SDS-PAGE. Protein was electroblotted on PVDF membrane at 100 V for 1h at 4 °C. Following the transfer, the membrane was blocked with 5% blocking buffer (5% non-fat dried milk and 0.1% Tween-20 in PBS) for 1 h at room temperature. The membrane was incubated overnight with specific primary antibody. After incubation membrane was washed three times with PBS-T (PBS containing 0.1% Tween 20) for 10 min and incubated with a secondary antibody at room temperature for 1 h. The membrane was washed three times with PBS-T and signal visualized by using EZ-ECL chemiluminescence detection kit for HRP (Takara, Japan) by exposing to X-ray film.

2.6. Isolation of mitochondria (MT), mitoplast (MP)and inter membrane space (IMS)

Mitochondria were isolated using Qproteome Mitochondria Isolation Kit (Qiagen, USA). Briefly, the cells ($7 X 10^6$) were resuspended in 700 μl lysis buffer. The cells were disrupted in disruption buffer using 24G needle and centrifuged at $1000\times g$ for 10 min at 4 °C and supernatant was collected. The mitochondrial fraction was collected by centrifugation at $6000\times g$ for 10 min at 4 °C and purified from the interface of disruption buffer and purification buffer. To prepare mitoplasts, the mitochondria were incubated in 10 mM potassium phosphate buffer supplemented with 2.7 mg/ml digitonin for 20 min in ice followed by centrifugation $10000\times g$ for 10 min at 4 °C. Supernatant containing IMS (intermembrane space) fraction was collected in other tube and the obtained mitoplast pellet was then washed thrice with PBS [23].

2.7. RNase treatment

The purified mitochondria were treated with RNase A (40 μg/ml) to remove bound non-specific RNA at 37 °C for 1 h in 300 μl buffer P1 (QIAprep Spin Miniprep Kit, Qiagen, USA) followed by treatment with 100 mg/ml proteinase K to stop the reaction.

2.8. miRNAs expression analysis by next generation sequencing and qPCR

Next generation sequencing (NGS) was performed to investigate mitochondrial and cellular miRNAs expression in HEK293 cells transfected with expanded CGG repeats. Small RNAs were isolated using miRCURY™ RNA Isolation Kit (Exiqon). Total RNAs were normalized using DESeq2 method followed by cDNA library preparation. QC analysis of library further confirms purity and integrity of RNAs. RNA samples were analyzed on Illumina HiSeq platform. For qPCR expression analysis, total RNAs were isolated using TRIzol reagent (Takara, Japan). Poly-A tailing of small RNA was done using *E. coli* Poly-A Polymerase (New England Biolabs, UK) at 37 °C for 20min, enzyme inactivation at 65 °C for 5 min followed by cDNA synthesis using cDNA synthesis kit (Takara, Japan).The cDNAs were synthesized using oligo dTs from same kit in two steps. For, miRNA expression analysis in FXTAS patients, the same RNAs were used which was mentioned in the previous study [15]. Primers for miRNAs were designed as previously [24].The levels of target transcripts were determined by $2^{-\Delta\Delta Ct}$ method using suitable endogenous control whereas 5S rRNA/U6 snRNA were endogenous controls for miRNA analysis. The reaction conditions were 95 °C for 2 min followed by 35 cycles of 95 °C for 5sec and 60 °C for 34 s (for mRNA)/1 min (for miRNA) (the data was acquired at this step).The melt curves were also acquired.

2.9. Droplet digital PCR workflow

EvaGreen chemistry was used for all the ddPCR performed in the study. Primer optimization and annealing temperature was standardized for all the targets. cDNA concentration was also optimized for each experiment to maintain ratio of positive and negative population to follow Poisson's distribution at 95% confidence of upper limit. A no template control (NTC) was included in every assay. Briefly, each ddPCR system of 20 μl was loaded into a disposable droplet generator cartridge (BioRad) followed by addition of 70 μl of droplet generation oil for EvaGreen (Bio-Rad)into each of the eight oilwells. The droplets were

generated by QX200 droplet generator (Bio-Rad) and transferred toa 96-well PCR plate (Bio-Rad) and the plate was heat-sealed with foil and placed in a conventional thermal cycler (Bio-Rad). The PCR condition for EvaGreen assays were as follows: 95˚C for 5 min, then 40 cycles of 95˚C for 30 s and 58˚C (depending on annealing temperature) for 1 min, and three final steps at 4˚Cfor5 minutes, 90˚C for 5 min, and a 4˚C for 30 min to enhance dye stabilization [25]. After completion of PCR cycle
plate was kept in QX200™ Droplet Reader and analyzed further using QuantaSoft™ software. The results were plotted in two ways by showing Ch1Amplitute and copies/µl, where yellow lines suggest partitions of droplets for each group which is also denoted by curly braces at the top. There are two population of droplets, (1) blue droplets, which are positive droplets for their respective targets and (2) grey droplets, which are negative droplets showing absence of their respective target (droplets which appear black are just bunch of grey droplets). Pink line in the graph indicates threshold intensity (Ch1: green) set to discriminate positive and negative droplets.

2.10. ATP levels

Cellular ATP levels were measured using ATP determination kit (Molecular Probes/Life Technologies, Canada) by adding 10 µl cell lysate in 100 µl ATP determination master mix containing 25 mM Tricine buffer, pH 7.8, 5 mM MgSO4, 0.5 mM D-luciferin, 1.25 µg/mL firefly luciferase, 100 µM EDTA and 1 mM DTT. The luminescence intensity was measured using TriStar^2 LB 942 Multimode Microplate Reader, Berthold Technologies, Germany. Protein content was determined by Bradford assay in each assay for normalization.

2.11. BN-PAGE and in-gel activity

The effect of miR-320a in premutation condition on mitochondrial complex-I and complex IV activity was determined by Blue native PAGE followed by In-gel activity [26]. Briefly, HEK293 were seeded at the density of 3 X 10^6 in 10 cm dishes, transfected with pEGFP-C1 (control) and5′UTR *FMR1* CGG99X along with mimic of miR-320a and control mimic. After 24 h of transfection, cells were collected, and mitochondrial fractions were isolated as described above using Qproteome Mitochondria Isolation Kit (37612, QIAGEN). 50 µg of mitochondrial protein for each condition was solubilized in solubilization buffer (50 mM NaCl, 50 mM Imidazole/HCl pH 7.0, 2 mM 6-aminohexanoic acid, 1 mM EDTA,6.0 g/g digitonin (10%)) and kept on ice for 30 min. After incubation, solubilized mitochondria were centrifuged for 20 min at 20, 000g. 20 µl supernatant was mixed with 3 µl 50% glycerol and 2 µl of 5% Coomassie blue G-250 (8 g/g detergent to dye ratio). The sample was loaded to 3-12%acrylamide gradient gel for BN-PAGE, run at room temperature and in-gel activity for mitochondrial complex I and complex IV was performed as described earlier [26].

2.12. ROS estimation

To determine ROS levels, cells were stained with CM-H_2CFDA (10 µM) for 15 min followed by quantification at 510/570–600 nm (ex/em) by fluorimeter (Hitachi High-Technologies Corp., Japan). The protein content was determined by Bradford assay in each assay for normalization.

2.13. Bioinformatics analysis and validations

The putative targets of altered miRNAs including miR-320a from Next Generation Sequencing (NGS) data were analyzed by miRDB and StarBase [27,28]. The targets with present in more than two target prediction software were shortlisted and submitted to DAVID annotation platform for clustering into meaningful groups [29]. The miRNAs which were showing high relevant targets to mitochondria, cell death and neuronal functions were selected for qPCR validation.

2.14. Statistical analysis

Most of the statistical tests and graphs of the results are generated by GraphPad Prism: version 7. Experimental data are shown as mean ± SEM for the number of observations. Student's unpaired *t*-test was performed wherever comparisons of two groups for repeated measurements to determine the levels of significance for each group. One-paired ANOVA test is used to calculate degree of significance wherever there are more than two groups (Dunnett's multiple comparison test).Each experiment has been repeated minimum two times independently and probability values of $p < 0.05$ were considered as statistically significant.

3. Results

3.1. Expression of expanded CGG repeats is toxic in different cell lines

Previous reports have suggested that expression of expanded CGG repeats embedded within the 5′UTR of *FMR1* shows cytotoxic effects in cell and animal models [6,30]. Therefore, to explore CGG repeats induced toxicity, we transfected plasmids expressing 99CGG repeats embedded at 5′UTR in the natural sequence of the human *FMR1* (Fig. 1A) into HEK293 (human embryonic kidney), SH-SY5Y (human neuroblastoma) and U87MG (human glioblastoma) cells. The expression of expanded CGG repeats in all cellular subtypes impairs mitochondrial metabolism as evident by XTT tetrazolium reduction assays (Fig. 1B, C, D). Furthermore, propidium iodide staining also indicated decreased cell viability in the cells transfected with expanded CGG repeats as compared control (Fig. 1E, F, G). Of interest, expression of ATG FMRpolyG-GFP, a construct with mutation of the natural non-canonical ACG start codon of FMRpolyG into an ATG canonical start codon enhanced FMRpolyG expression and results into reduced metabolism and increased cell death. As a positive control, we used H_2O_2 treatment to induce cell death [31]. Overall, these results are consistent with previous reports [9,15, 32], and confirm that expression of CGG repeats alters cellular metabolism and promotes cellular toxicity in cells from different origin.

3.2. Expanded CGG repeats alter miRNAs expression and their association with mitochondria

Growing evidences suggest that specific miRNAs can be present in specific membrane-bound compartments including secreted vesicles, ER membrane and mitochondria [18,20,33–35]. As miRNAs expression and mitochondrial functions are affected in FXTAS, we investigated the association of miRNAs with mitochondria in premutation condition. Briefly, small RNAs were isolated from mitochondrial fractions and total cell of HEK293 cells transfected with ATG FMRpolyG-GFP, 5′UTR *FMR1* CGG99X and pEGFP-C1. RNA samples were analyzed on Illumina HiSeq platform by following standard method (Fig. 2A). The RNA sequencing results showed down regulation of a majority of miRNAs in both ATG FMRpolyG-GFP and 5′UTR *FMR1* CGG99X transfected conditions in mitochondrial and total cell fractions (Fig. S1 A, B, C, D), which is consistent with previous studies [20,36], and validates our experimental strategy. We further confirmed decreased levels of candidate miRNAs in RNAs isolated from brain tissue of individuals with FXTAS compared to control (Fig S1 E). Interestingly, high reads of some specific miRNAs from the mitochondrial fractions indicated their enhanced association with mitochondria in premutation conditions (Fig. 2 B, C). We also observed that some miRNAs showing reduced reads in total cells, were highly enriched in mitochondrial fraction and vice versa in both CGG repeats transected groups (Fig. 2 D, E). Further, there were some miRNAs which showed no significant change in terms of their abundance in total cell lysates but showed altered pattern of association with mitochondria (Fig. 2F and G).

The putative targets of these miRNAs associated to mitochondria in FXTAS condition were enlisted by using miRDB [27]. The targets were

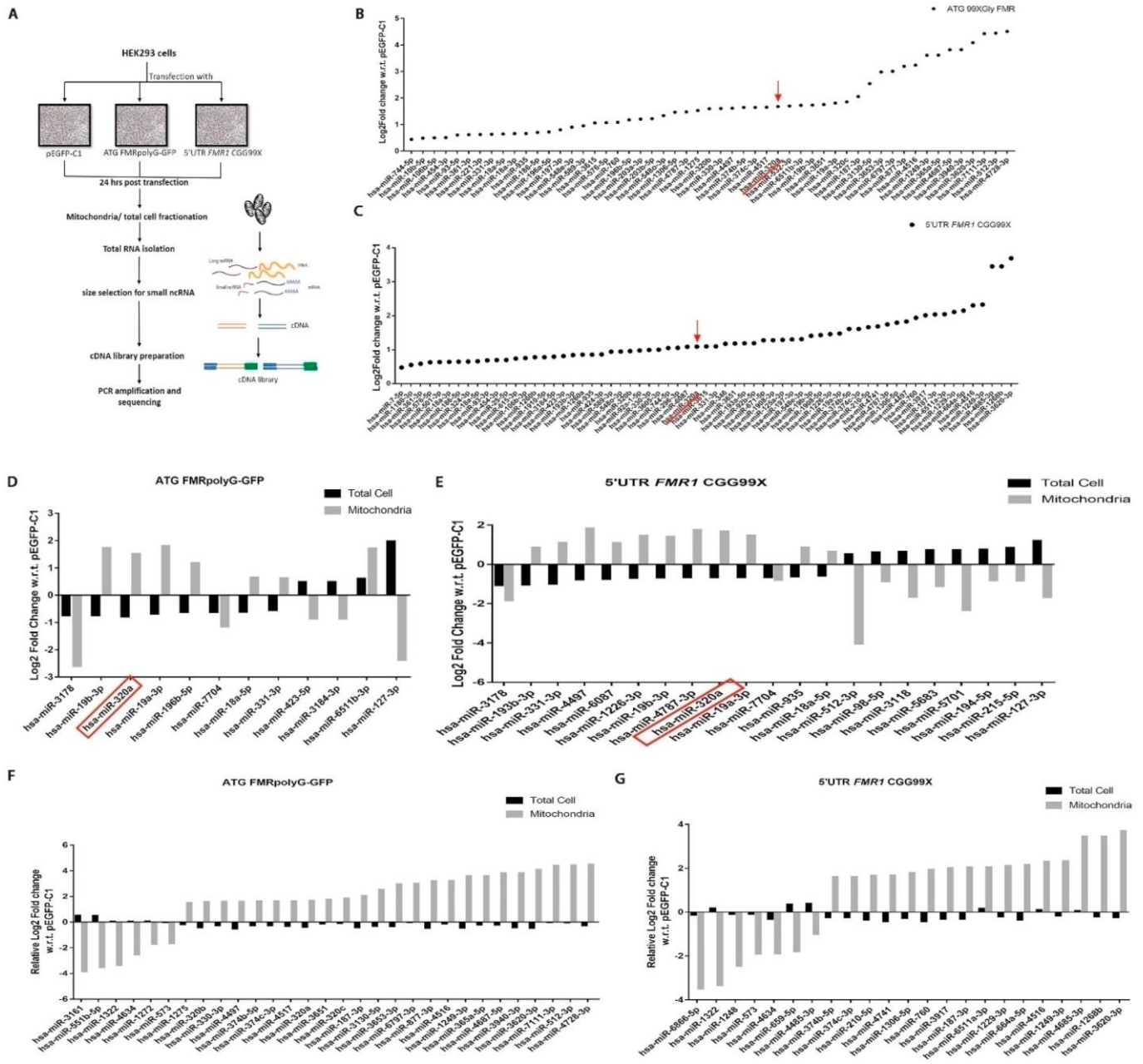

Fig. 2. FMRpolyG translated due to CGG repeats causes altered pattern of mitochondrial associated miRNAs. Flowchart explaining workflow beginning with transfection of premutation constructs followed by mitochondrial fractionation and isolation of RNAs for next generation sequencing (A). NGS analysis showing high expression levels of miRNAs in mitochondrial fraction of HEK293 cells transfected with ATG FMRpolyG-GFP (B) and 5′UTR*FMR1* CGG99X (C) compared to pEGFP-C1 (See also Fig. S1 A, B for list of miRNAs altered in total cell fraction and Fig. S1 C, D for miRNAs showed low enrichment in mitochondria). Representative graphs showing opposite enrichment of miRNAs in mitochondrial and total cell fraction under ATG FMRpolyG-GFP (D) and 5′UTR*FMR1* CGG99X (E) transfected condition. Comparative analysis for miRNAs enrichment which remained unchanged in total cell fraction while showed altered pattern of association at mitochondria in ATG FMRpolyG-GFP (F) and 5′UTR*FMR1* CGG99X (G)transfected condition. ($n = 2$, for all the listed miRNAs p and $p_{adj} \leq 0.05$).

clustered into different useful groups such as OMIM enriched tissue, biological process and cellular compartments using DAVID platform [29]. The bioinformatics analysis for tissue enrichment showed that 37% and 40% of the targets of mito-miRs from transfected ATG FMRpolyG-GFP (Fig S2 A) and 5′UTR *FMR1* (CGG)99X (Fig S2 B) were associated with brain, respectively. Clustering based on biological process indicates involvement of targets in nervous system development, mRNA processing, protein ubiquitination and other neuronal functions (Fig. S2 C, D). In addition, clustering based on cellular compartments, reveals association of targets with axon, dendrites, synapse and post synaptic membrane (Fig. S2 E, F). These bioinformatics analysis suggests that a specific population of miRNAs translocates to mitochondria under FXTAS condition and their targets are associated with brain and neuronal functions.

3.3. *Mito-miR, miR-320a translocates to mitoplast in FXTAS condition*

The altered pattern of association of miRNAs with mitochondria in premutation condition was further confirmed by qRT-PCR. U6 snRNA and 5S rRNA were evaluated for reference RNA and positive control for mitochondrial fraction as both of them have been reported to associate with mitochondria [36,37]. We observed no change in the Ct values of

5S rRNA in mitochondria, cytosol and WCL between control and CGG repeats transfected groups. Ct values of U6 snRNA were notably altered in control and CGG repeats transfected groups in all sub cellular fractions (Fig. S3A). 5S rRNA was used as reference RNA for several reasons as 5S rRNA has been known to be transcribed in the nucleus and transported to mitochondria and associates with mitochondrial ribosomes [38,39]. Further, the miRNA of our interest miR-320a, is also nuclear encoded and transported to mitochondria under CGG repeat transfected conditions. Hence, to rule out any transport defect, 5S rRNA was selected as endogenous control to compare the change in expression levels of miRNAs under premutation condition for all subcellular fractions. Candidate miRNAs hsa-miR-181a, hsa-miR-221, hsa-miR-320a, hsa-miR-4485 and hsa-miR-148-3p were selected for their quantification in whole cell, mitochondria and cytosolic fractions from HEK293 cells transfected with ATG FMRpolyG-GFP, 5′UTR *FMR1* CGG99X and pEGFP-C1. The selected miRNAs showed differential pattern of association with mitochondria as compared to their whole cell enrichment in premutation condition (Fig. 3A). We selected miR-320a for further exploration as this miRNA was previously reported as a mito-miR [35, 40], and its protective roles during cellular stress and a tumor suppressor have been reported in some studies [41,42]. mito-miRs can possibly localize in submitochondrial compartments; hence, submitochondrial localization of miR-320a was analyzed by isolating pure fractions of mitochondria, mitoplast and intermembrane space (IMS) and analyzing the level of miR-320a. Immunoblotting against TOMM20, a marker of the outer membrane protein showed high level in mitochondria and IMS fractions but not in mitoplast. AIF, a marker of the mitochondrial inner membrane was found in mitochondria and mitoplast, confirming the purity of the submitochondrial fractions (Fig S3 B). The purity of submitochondrial fractions was further confirmed by estimating levels of different RNAs including actin (cytosol), COX1 (mitoplast) and miR-4485 (mitoplast [20]). where corresponding low Ct value of actin in total cell as compared to other sub mitochondrial fractions and low Ct values of COX1and miR-4485 in submitochondrial fractions as compared to total cell suggest purity of submitochondrial fraction at RNA level (Fig S3 C). RNase A protection assay was performed with mitochondria and mitoplast fractions from HEK293 cells followed by RNA isolation. qPCR analysis showed high levels of miR-320a in RNase A treated mitoplasts and was not degraded upon treatment with RNase A suggesting its localization in mitoplast (Fig. 3B).

ddPCR can determine copy number of RNA accurately and has been proved to be more tolerant to the presence of inhibitors of the

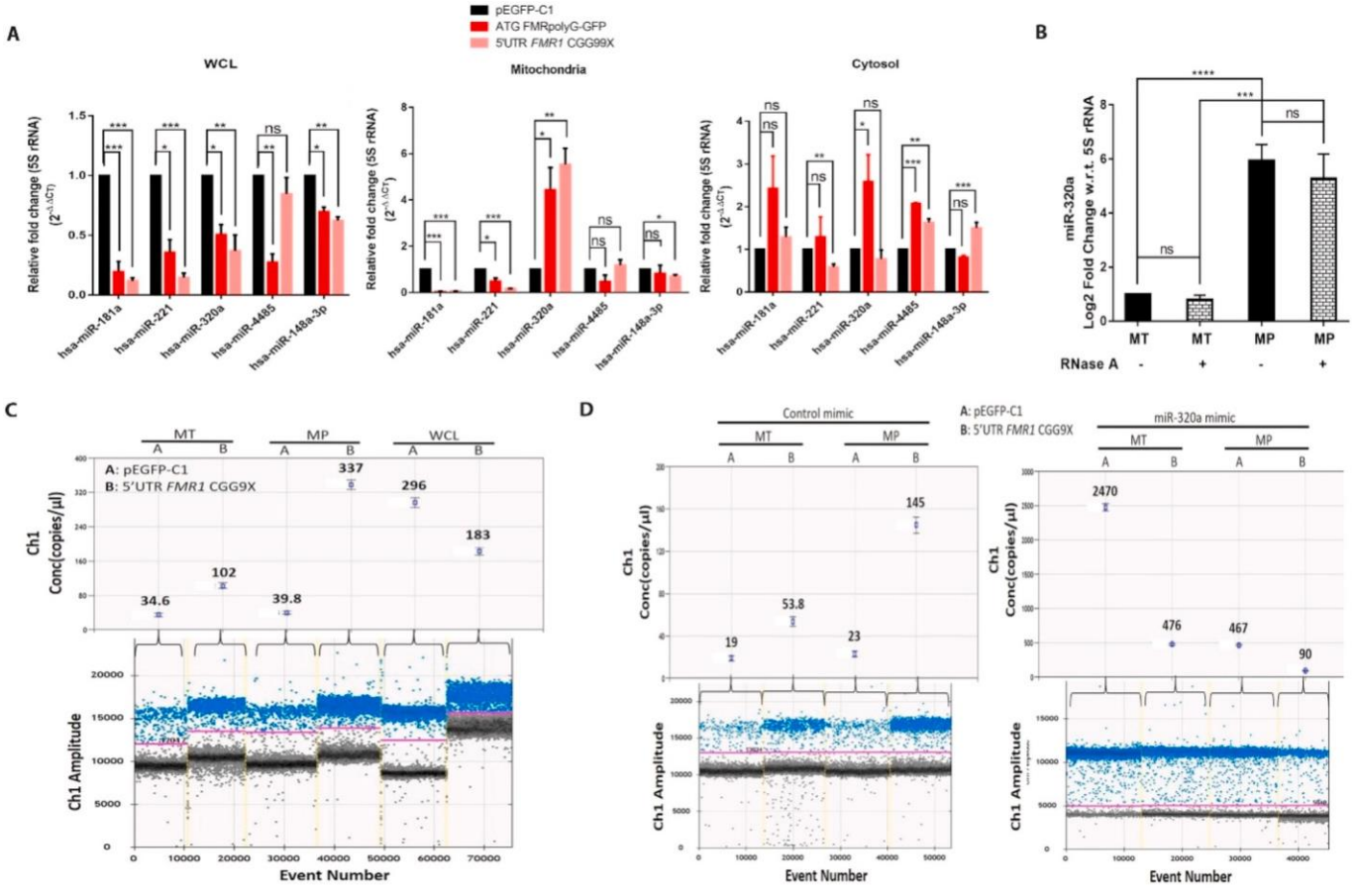

Fig. 3. Validation of candidate miRNAs by qPCR and localization of miR-320ain mitoplast under premutation condition. Candidate miRNAs has-miR-181a, hsa-miR-221, hsa-miR-320a,hsa-miR-4485 and hsa-miR-148a-3p were selected from the next generation sequencing analysis and their sub cellular localization was checked in various compartments such as whole cell lysate (WCL), mitochondria and cytosol under both CGG repeats transfected condition (n = 3, endogenous control: 5S rRNA) (A). Mitoplast fraction was prepared by treating mitochondria with digitonin and both mitochondrial and mitoplast fractions were treated with RNase A to confirm submitochondrial localization of miR-320a (n = 3)(B) (See also Fig. S3 B of western blotting and Fig. S3 C for qPCR validation showing purity of submitochondrial fractions). Digital Droplet PCR: droplet distribution and box plot representing enrichment of miR-320a in mitochondria (MT), mitoplast (MP) and whole cell lysate (WCL) under 5′UTR *FMR1* CGG99X transfected condition compared to control (n = 2, Blue: positive droplets, Grey: negative droplets, box plots represents concentration in copies/ul) (C), see also Fig. S3 D for qPCR validation of the same experiment. Enrichment of exogenously transfected miR-320a mimic at mitochondria and mitoplast represented as change in amplitude of positive droplets (blue) and altered copies/ul (box plot) under premutation condition (n = 3) (D), see also Fig. S3 E for qPCR validation for mitoplast enrichment of miR-320a under miR-320a mimic transfected condition. (For interpretation of the references to colour in this figure legend, the reader is referred to the Web version of this article.)

amplification reaction compared to qPCR [43]. These properties of ddPCR have made it useful for detection of cellular and circulating miRNAs [44]. We performed ddPCR to further quantify the changes in abundance of miR-320a in mitochondria, mitoplast and whole cell fractions. Increased number of positive droplets (blue) and more copies/µl of miR-320a was observed in mitochondria and mitoplast fraction in 5′UTR *FMR1* CGG99X transfected condition as compared to pEGFP-C1 (Fig. 3C, S3 D). The results were consistent with RT-qPCR results as observed in Fig. 3A. Furthermore, ddPCR confirmed decreased levels of miR-320a under premutation conditions in whole cell lysate (Fig. 3C). These results suggest that expression of CGG repeats may either induce degradation of miR-320a within the cytoplasm and/or enhance its translocation to mitochondria, inside the mitoplast. To discriminate between these hypothesis, we transfected HEK293 cells with a synthetic mimic of miR-320a along with a control for both pEGFP-C1 and 5′UTR *FMR1*CGG99X transfected conditions. The transfection of miR-320a mimic in cells showed enhanced localization of miR-320a in mitochondria as well as in mitoplast in 5′UTR

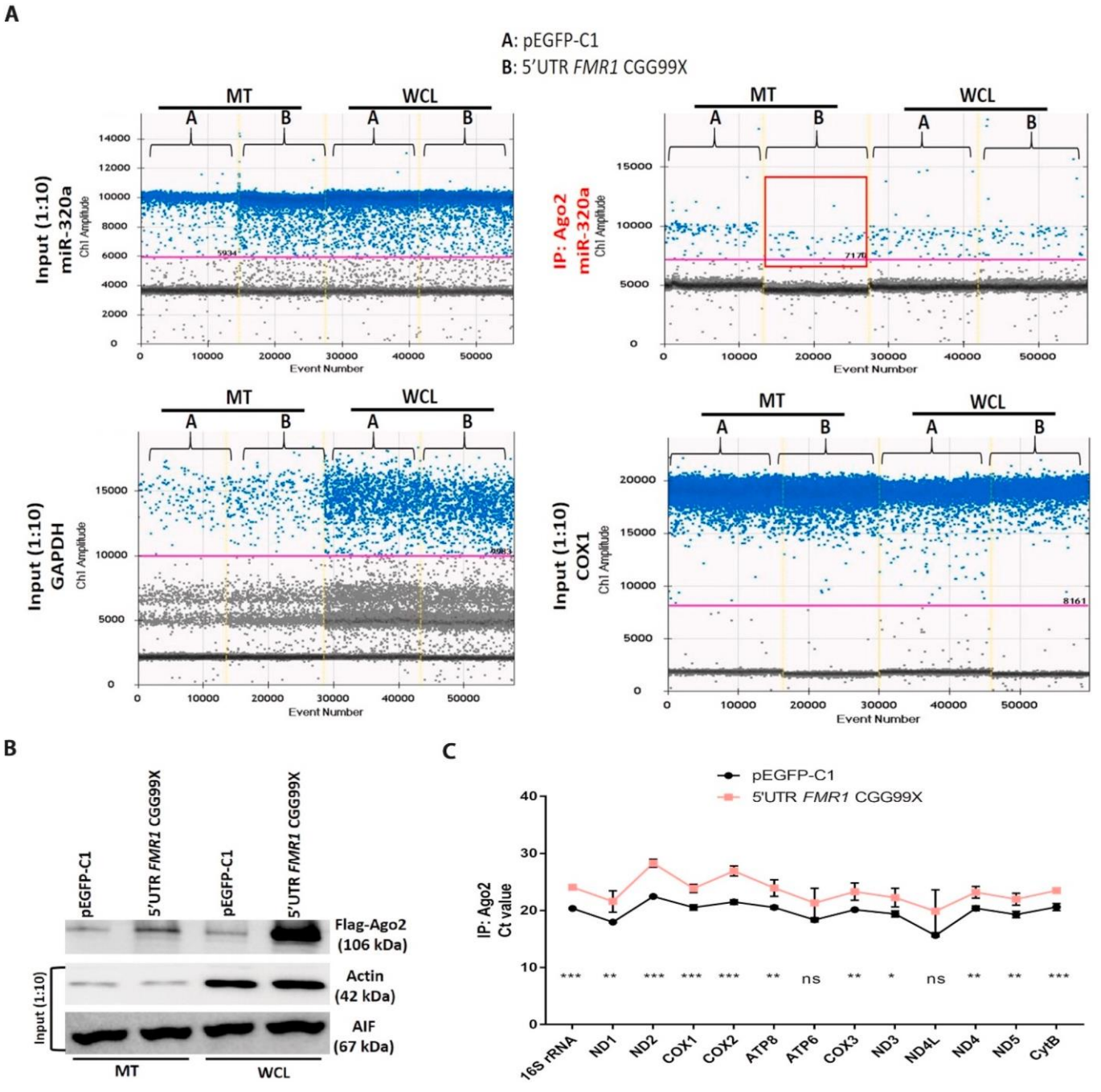

Fig. 4. miR-320a regulates levels of mitochondrial transcripts by modulating RISC assembly with Ago2 and mitotranscripts. Flag-Ago2 cotransfected with expanded CGG repeats and control. Equal amounts of purified mitochondria and whole cell lysate (WCL) were subjected to RNA immunoprecipitation using anti-flag beads. Population of miR-320a bound to Ago2 was determined using ddPCR. 1D plot for droplet distribution (A) indicates levels of miR-320a bound with Ago2 in premutation condition in both the fraction. Input (1:10) was analyzed for reference gene of mitochondria (COX1) and WCL (GAPDH) and to detect endogenous miR-320a levels, see also Fig. S4 A for box plots and Fig. S4 B for the same experiment validated by qPCR. Western blotting data showed specific anti-Ago2 IP blotted against flag antibody where Input (1:10) was probed against actin and AIF antibody for validation of mitochondrial fraction (B). Individual mitochondrial transcripts bound to miR-320a from RNAs of Ago-IP were examined by qPCR (plotted respective Ct values) (C). (n = 2) $p > 0.05$ (ns), $p \leq 0.05$ (*),$p \leq 0.01$ (**), $p \leq 0.001$ (***).

*FMR1*CGG99X condition as compared to control (Fig. 3D and S3D).Here, we observed that high proportion of endogenous miR-320a is enriched in mitoplast in control mimic transfected conditions in 5′UTR *FMR1*CGG99X transfected cells. Although, cells expressing 5′UTR *FMR1*CGG99X along with miR-320a mimic showed high copies/μl in mitochondria but the pattern of miR-320a translocation to mitochondria/mitoplast was not the same as observed in control mimic condition. Overall, these results suggest that miR-320a translocates to mitochondria and resides in mitoplast and this transport is enhanced in FXTAS condition.

3.4. miR-320a fails to form a functional RISC complex in mitochondria

The mitoplast enrichment of miR-320a suggest that it may regulate mitochondrial transcripts processing and/or translation. Therefore, to identify the role of miR-320a inside the mitoplast, we searched for putative targets of miR-320a by miRDB and StarBase. The list of potential mRNAs targeted by miR-320a comprises various nuclear encoded mitochondrial proteins, including EARS2, GLUD1, COX11, SDHC, SDHD, NDUFS1 and NDUFA10 (Table S2). Interestingly, we also identified putative miR-320a targets in multiple mitochondrial transcripts, including 16S rRNA, ND1, COX1, ND4, CytB and ND5 using BLASTn tool (Fig. S5).

Ago2 is an essential component of RISC and growing evidences suggest the presence of Ago2 inside mitochondria, where it may regulate expression of some mitochondrial transcripts [45–47]. Thus, to test whether miR-320a may assemble in a RISC-like complex with Ago2 and regulate mitotranscripts, we first tested the possible binding of miR-320a with Ago2 by RNA-immunoprecipitation assay followed by ddPCR. Analysis of RNA-IP showed less population of miR-320a positive droplets (blue) (Fig. 4A) and decreased copy number/μl (Fig. S4A) in the mitochondrial fraction of CGG repeats transfected cells as compared to control. Similar results were obtained by RT-qPCR (Fig. S4B). COX1, which is mitochondrial genome encoded transcript was used as endogenous control as well as reference RNA to check purity of mitochondrial fraction. COX1 has already been shown no change in its levels upon expression of expanded CGG repeats in HEK293 cells [15]. High abundance of positive droplets of COX1 (input) and low number of GAPDH (input) positive droplets confirmed purity of mitochondrial fractions. Interestingly, immunoblotting analysis showed increased level of Ago2 in total cell lysate as well as in mitochondria in the cells expressing of 5′UTR *FMR1* CGG99X (Fig. 4 B). Finally, RT-qPCR of various mitochondrial transcripts were performed using RNAs of Ago2-IP from the mitochondrial fraction to estimate the levels of mitotranscripts bound to Ago2 upon expression of 5′UTR *FMR1* CGG99X as compared to control pEGFP-C1. The higher Ct values for majority of mitochondrial transcripts revealed a decreased binding of mitotranscripts with Ago2 in premutation condition as compared to control (Fig. 4C). Collectively, our data suggests an increased translocation of miR-320a as well as of Ago2 into mitochondria under premutation condition; however, this

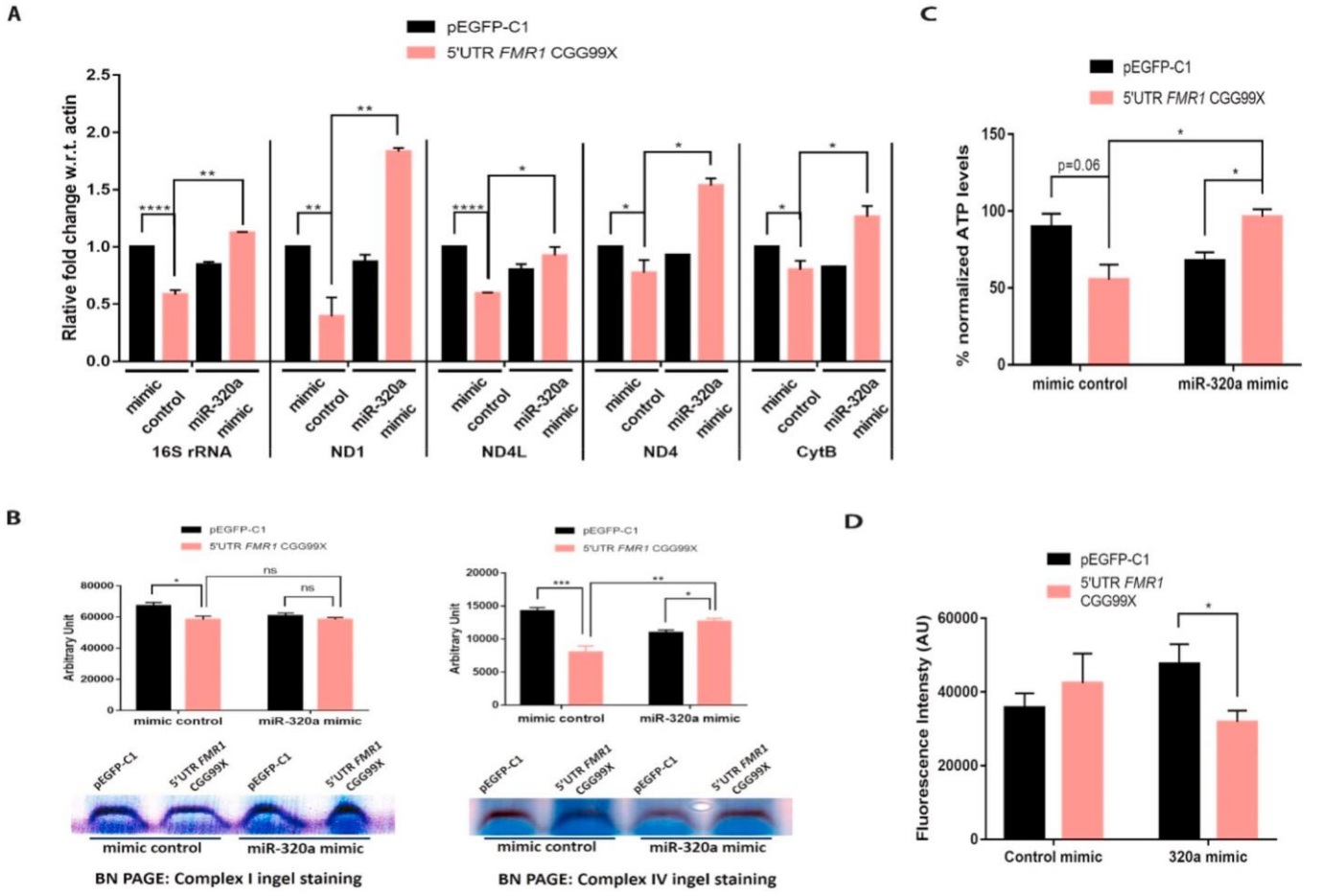

Fig. 5. Rescued mitochondrial transcripts due to miR-320a led to enhanced mitochondrial functions in FXTAS. HEK293 cells transfected with miR-320a mimic along with 5′UTR *FMR1* CGG99X and pEGFP-C1. After 24 h of transfection, mitochondrial functions have been analyzed. qPCR results showing levels of mitochondrial transcripts influenced by miR-320a mimic. endogenous control: actin (n = 4) (A). Effect of miR-320a mimic on activity of mitochondrial complex I and IV determined by BN PAGE followed by ingel staining (includes densitometry analysis, n = 3) (B). ATP levels were also monitored within same groups (n = 3) (C). Cellular ROS levels were determined by staining the cells with H_2DCFDA and fluorescence intensity was plotted for each group (n = 3, Rotenone; positive control) (D).p > 0.05 (ns), p ≤ 0.05 (*),p ≤ 0.01 (**), p ≤ 0.001 (***).

does not result in assembly of a functional RISC like complex.

3.5. *miR-320a improves mitochondrial transcripts levels and mitochondrial functions in FXTAS conditions*

To understand the impact of the decreased binding of miR-320a with Ago2 on mitochondrial functions, we first quantified the level of mitochondrial transcripts in FXTAS condition. The expression of 5′UTR *FMR1* CGG99X showed decreased levels of mitotranscripts (Fig. 5A), which is consistent with previous reports [12,15]. Interestingly, we observed a rescue in levels of majority of mitotranscripts in presence of miR-320a mimic (Fig. 5A). Next, we explored the effect of CGG repeats and miR-320a on the activity of mitochondrial respiratory chain. Briefly, HEK293 cells were transfected with pEGFP-C1 and 5′UTR *FMR1* CGG99X along with miR-320a mimic and mitochondrial fractions were isolated. BN PAGE was performed followed by in-gel staining for complex I and IV. Expression of the CGG premutation significantly decreased complex I (NADH dehydrogenase) and complex IV (Cytochrome Oxidase) activities compared to control condition (Fig. 5B). Importantly, cotransfection with miR-320a mimic corrects the deleterious effect of the CGG repeats on complex IV activity (Fig. 5B). Further, transfection of miR-320a mimic enhanced the level of ATP in cells expressing 5′UTR *FMR1* CGG99X (Fig. 5C). Finally, we examined cellular ROS levels by DCFDA staining where rotenone (25 μM for 2 h) treated group taken as positive control. The increased ROS levels in premutation condition was not statistically significant; however, cotransfection with miR-320a mimic caused decreased levels of cellular ROS under 5′UTR *FMR1* CGG99X (Fig. 5D). Combining all the results, it can be inferred that miR-320a can rescue some of the mitochondrial dysfunctions in FXTAS condition.

3.6. *miR-320a improves cell survival in FXTAS condition*

To investigate whether the improved mitochondrial functions mediated by miR-320a also impacts cell viability, HEK293 cells were co-transfected with plasmid 5′UTR *FMR1* CGG99X along with miR-320a mimic followed by propidium iodide (PI) and MTT staining. Importantly, 5′UTR *FMR1* CGG99X cotransfected with miR-320a mimic showed decreased level of PI fluorescence, indicating decreased cell death as compared to CGG repeats transfected with control mimic (Fig. 6A). Similarly, MTT assay indicated increased cellular viability in presence of miR-320a mimic in CGG repeat transfected cells (Fig. 6B). We also monitored PARP cleavage and caspase activation by western blotting. As expected, increased PARP and caspase 3 cleavage were observed in premutation conditions which is in consonance with earlier findings [13,15]. Further, the level of cleaved PARP and active caspase 3

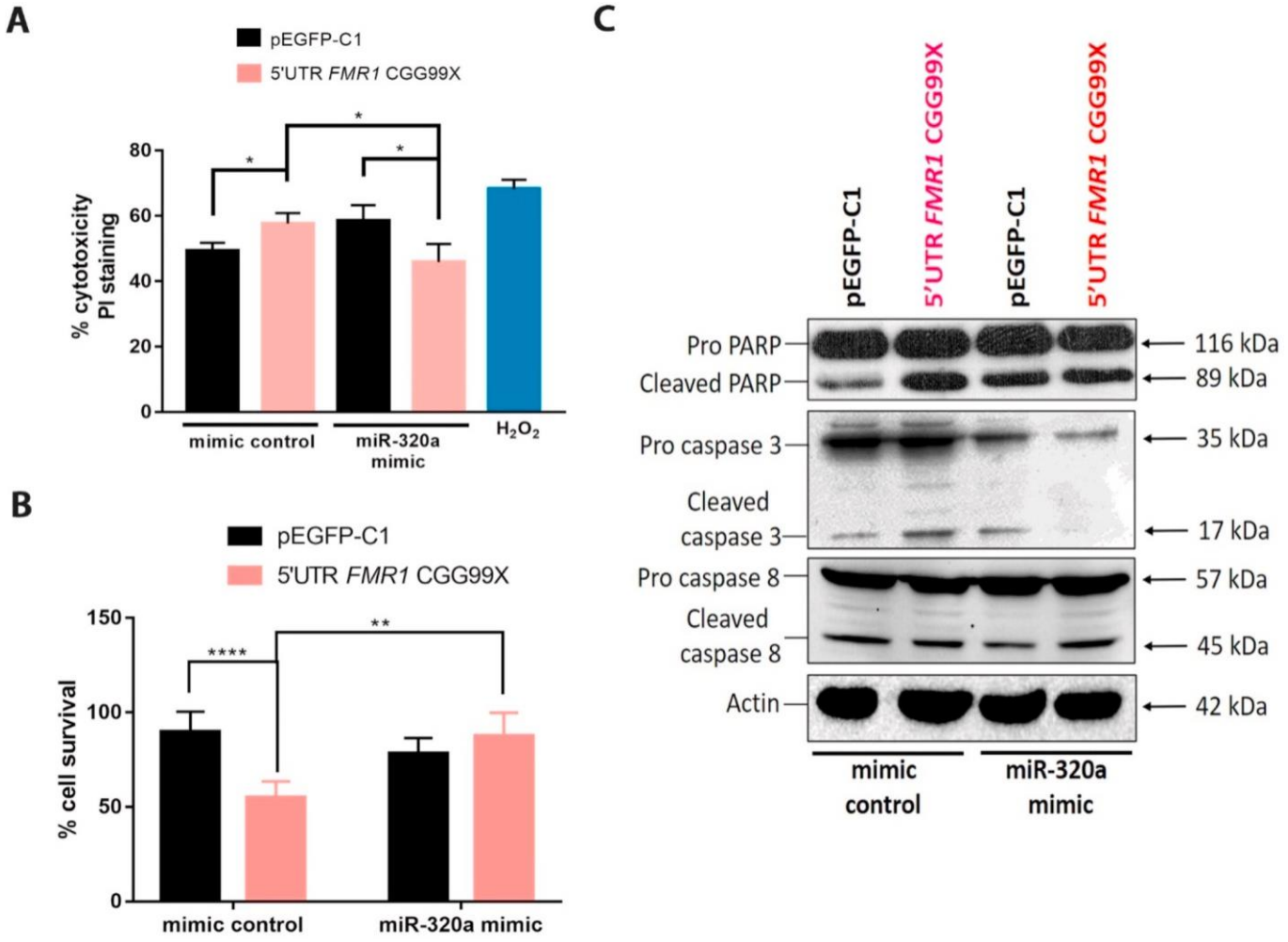

Fig. 6. miR-320a causes decreased cellular ROS levels and increased survival in premutation condition. Cytoprotective role of miR-320a was analyzed by transfecting miR-320a under CGG repeats expressed condition together with respective controls in HEK293 cells. PI staining was performed to assay population of cells undergoing apoptosis (n = 3, H_2O_2:positive control) (A). Recued cell death and increased cell survival was investigated by MTT assay (n = 3) (B). Western blotting was performed by probing and detecting the samples against different apoptotic markers such as caspase 3, caspase 8 and PARP (n = 3) (C). $p > 0.05$ (ns), $p \leq 0.05$ (*),$p \leq 0.01$ (**), $p \leq 0.001$ (***).

decreased in cells expressing CGG repeats in presence of miR-320a mimic(Fig. 6C). Collectively, these data indicate that miR-320a can improve cell viability in *in vitro* cellular model of FXTAS.

4. Discussion

Mitochondrial dysfunction is a key pathogenic event reported in FXTAS cellular and animal models and premutation carriers [8,11,30,31,48]; however, the molecular mechanism causing such mitochondrial dysfunctions in FXTAS remain to be determined. The plausible hypothesis behind such mitochondrial dysfunctions can be titration of DROSHA and DGCR8 by the expanded CGG repeats RNA resulting in decreased miRNA biogenesis [20].This is consistent with our miRNA expression data in FXTAS patients, where we observed decreased miRNA levels in RNAs derived from brain tissue of premutation carriers. Furthermore, FMRP, the protein encoded by *FMR1*, is known to regulate mRNA translation via interacting with Dicer in the RISC. Therefore, decreased levels of FMRP observed in premutation carriers may also affect miRNA function by altering RISC activity [49,50]. We recently reported that FMRpolyG transiently interacts with mitochondria and alter mitochondrial functions [15] and an earlier mass spectroscopy analysis of FMRpolyG interacting proteins identified several proteins important for nuclear-cytoplasmic trafficking but also for mitochondrial RNA processing (FASTKD5,DHX30) [29]. This suggests that FMRpolyG may not only alter pre-miRNAs export from the nucleus, but also proteins important for the import and processing of miRNAs within mitochondria. This hypothesis is in consonance with our current work where we observed decreased cellular miRNAs and their altered translocation to mitochondria. This may have large pathogenic consequences, as bioinformatics analysis indicated that targets of identified mito-miRs are involved in regulation crucial neuronal and mitochondrial functions; however, this hypothesis needs to be formally addressed, especially as the molecular mechanism for transport of miRNAs to mitoplast is unclear [51].

Our group has previously reported that miRNAs can translocate to mitochondria under different patho-physiological stimuli [16,43]. The transport of nuclear encoded miRNAs to the mitochondria is required for optimal mitochondrial function [36,47]. There can be multiple pathways by which miRNAs residing in mitochondria can regulate mitochondrial functions. First, miRNAs can directly bind to mito-DNA and can regulate transcription of mitogenome [40,52]. Second, miRNAs can affect RNA processing causing RNA interference by binding to immature mitotranscripts [20]. Third, miRNAs can regulate translation of mature transcripts by forming RISC like assembly with Ago2 within mitochondria and interfere with mito-ribosome scanning [47,48]. The evidences here along with previous reports strengthen the hypothesis of presence of Ago2, component of RISC inside the mitochondria; while presence of full RISC complex is still elusive. Interestingly RNA-IP with Ago2 showed miR-320a interaction with mitochondrial transcripts supports the earlier findings claiming Ago2 binds to miRNA-mito transcripts and regulate the mitochondrial translation [47].

We identified a population of miRNAs which associates with mitochondria due to cellular stress induced by expression of 5′UTR *FMR1* CGG99X which might be involved in restore of mitochondrial functions. Among these miRNAs, we characterized miR-320a for its functional role in FXTAS. RNase A protection assay along with ddPCR confirmed the presence of miR-320a within mitoplast. RNA-IP with Ago2 suggest decreased loading of miR-320a with mitochondrial transcript and Ago2 in FXTAS condition. Interestingly, transfection of miR-320a mimic positively modulates mitotranscripts processing and ultimately restores mitochondrial functions in premutation condition. This clearly suggests that miRNA-mitotranscripts interaction with Ago2 may regulate the level of mitochondrial DNA encoded proteins in narrow physiological range for maintaining optimal functions (graphical abstract). This study provides better understanding of the underlying molecular mechanism by which miRNAs can associate with mitochondria in complicated pathology like FXTAS and other chronic neurodegenerative conditions. This can be an important finding that may help to develop mito-miR based approaches to rescue the mitochondrial symptoms in FXTAS condition.

Author contributions

Gohel D: Performed experiments, Investigation, validation, writing-original draft.

Sripada L, Prajapati P, Currim F, Roy M, Singh K, Shinde A, Mane M, Kotadia D, Tassone F, Berguerand NC: Formal data analysis, methodology, resources.

Singh R: Conceptualization, Methodology, Resources, Writing – original draft, Visualization, Supervision, Funding acquisition.

Declaration of competing interest

The authors declare no competing interests.

Acknowledgements

The current research work was financially supported by the Department of Science and Technology, Government of India, Indo-French grant (DST/ANR2014/Neuro-1/FXTAS) to Prof. Rajesh Singh (Indian investigator) and Dr. Nicolas Charlet Berguerand (French investigator). This work constitutes part of the Ph.D. thesis of Dhruv Gohel who received Senior Research fellowships from Indian Council of Medical Research (ICMR), India. Authors acknowledge the FIST program supported by DST, Government of India. Authors also acknowledge the DBT-MSUB-ILSPARE program of the Department of Biochemistry, The M S University of Baroda sponsored by DBT, Govt. of India.

Appendix A. Supplementary data

References

[1] R.J. Hagerman, et al., Fragile-X-associated tremor/ataxia syndrome (FXTAS) in females with the FMR1 premutation, Am. J. Hum. Genet. 74 (2004) 1051–1056, 0002-9297 (Print).
[2] A. James, et al., Fragile X Premutation Tremor/Ataxia Syndrome : Molecular , Clinical , and Neuroimaging Correlates Se, 2003, pp. 869–878.
[3] P.C. Population, et al., Penetrance of the fragile X – associated tremor/ataxia syndrome in a 291 (4) (2015).
[4] R.J. Hagerman, et al., Intention Tremor , Parkinsonism , and Generalized Brain Atrophy in Male, 2001.
[5] C. Sellier, et al., Article sequestration of DROSHA and DGCR8 by expanded CGG RNA repeats alters MicroRNA processing in fragile X-associated tremor/ataxia syndrome identification of proteins associated with expanded, Cell Rep. 3 (3) (2013) 869–880.
[6] H. Tan, M. Poidevin, H. Li, D. Chen, P. Jin, MicroRNA-277 modulates the neurodegeneration caused by fragile X premutation rCGG repeats 8 (5) (2012).
[7] E. Martí, M. Mil, MicroRNA Expression Profiling in Blood from Fragile X-Associated Tremor/ataxia Syndrome Patients, 2013, pp. 595–603.
[8] S.Y. Fxtas, P.J. Hagerman, R.J. Hagerman, F X-A T/a S (Fxtas), vol. 30, 2004, pp. 25–30, no. May 2003.
[9] C. Sellier, et al., Translation of Expanded CGG Repeats into FMRpolyG Is Pathogenic and May Contribute to Fragile X Tremor Ataxia Syndrome Article Translation of Expanded CGG Repeats into FMRpolyG Is Pathogenic and May Contribute to Fragile X Tremor Ataxia Syndrome, 2017, pp. 331–347.
[10] P.K. Todd, et al., Article CGG repeat-associated translation mediates neurodegeneration in fragile X tremor ataxia syndrome, Neuron 78 (3) (2013) 440–455.
[11] V. Nobile, et al., Altered mitochondrial function in cells carrying a premutation or unmethylated full mutation of the FMR1 gene, Hum. Genet. 139 (2) (2020) 227–245.
[12] C. Ross-Inta, et al., Evidence of mitochondrial dysfunction in fragile X-associated tremor/ataxia syndrome, Biochem. J. 429 (3) (2010) 545–552.
[13] R.K. Hukema, et al., Induced expression of expanded CGG RNA causes mitochondrial dysfunction in vivo, Cell Cycle 13 (16) (2014) 2600–2608.

[14] I. Madrigal, G. Garrabou, M. Mil`a, Impaired mitochondrial function and dynamics in the pathogenesis of FXTAS, Mol. Neurobiol. 54 (2016) 6896–6902.
[15] D. Gohel, L. Sripada, P. Prajapati, K. Singh, M. Roy, BBA - molecular Basis of Disease FMRpolyG alters mitochondrial transcripts level and respiratory chain complex assembly in Fragile X associated tremor/ataxia syndrome [FXTAS], BBA - Mol. Basis Dis. 1865 (6) (2019) 1379–1388.
[16] M. Chekulaeva, W. Filipowicz, Mechanisms of miRNA-mediated post-transcriptional regulation in animal cells,, Curr. Opin. Cell Biol. 21 (3) (2009) 452–460.
[17] R.W. Carthew, E.J. Sontheimer, Origins and Mechanisms of miRNAs and siRNAs, Cell 136 (4) (2009) 642–655.
[18] S. Bandiera, R. Mat´egot, M. Girard, J. Demongeot, A. Henrion-caude, Free Radical Biology and Medicine MitomiRs delineating the intracellular localization of microRNAs at mitochondria, Free Radic. Biol. Med. 64 (2013) 12–19.
[19] S. Pitchiaya, et al., Resolving subcellular miRNA trafficking and turnover at single-molecule resolution article resolving subcellular miRNA trafficking and turnover at single-molecule resolution, Cell Rep. 19 (3) (2017) 630–642.
[20] L. Sripada, et al., hsa-miR-4485 regulates mitochondrial functions and inhibits the tumorigenicity of breast cancer cells, J. Mol. Med. 95 (6) (2017) 641–651.
[21] D. Jeandard, A. Smirnova, I. Tarassov, E. Barrey, A. Smirnov, N. Entelis, Import of non-coding RNAs into human mitochondria: a critical review and emerging approaches, Cells 8 (3) (2019) 286.
[22] P. Prajapati, L. Sripada, K. Singh, K. Bhatelia, R. Singh, R. Singh, Biochimica et Biophysica Acta TNF- α regulates miRNA targeting mitochondrial complex-I and induces cell death in dopaminergic cells, BBA - Mol. Basis Dis. 1852 (3) (2015) 451–461.
[23] K. Singh, L. Sripada, A. Lipatova, M. Roy, P. Prajapati, BBA - molecular Cell Research NLRX1 resides in mitochondrial RNA granules and regulates mitochondrial RNA processing and bioenergetic adaptation, BBA - Mol. Cell Res. 1865 (9) (2018) 1260–1276.
[24] I. Balcells, S. Cirera, P.K. Busk, Specific and sensitive quantitative RT-PCR of miRNAs with DNA primers, BMC Biotechnol. 11 (1) (2011) 70.
[25] G.P. Mcdermott, et al., Multiplexed Target Detection Using DNA- Binding Dye Chemistry in Droplet Digital PCR, 2013.
[26] P. Jha, X. Wang, J. Auwerx, Analysis of mitochondrial respiratory (BN-PAGE) 6 (March) (2016) 1–14.
[27] X. Wang, X. Wang, miRDB : A microRNA Target Prediction and Functional Annotation Database with a Wiki Interface miRDB : A microRNA Target Prediction and Functional Annotation Database with a Wiki Interface, 2008, pp. 1012–1017.
[28] S. Liu, H. Zhou, L. Qu, J. Yang, miRNA-ncRNA and Protein – RNA Interaction Networks from Large-Scale CLIP-Seq Data, 2013 no. December.
[29] D.W. Huang, B.T. Sherman, R.A. Lempicki, Systematic and Integrative Analysis of Large Gene Lists Using DAVID Bioinformatics Resources, 2008 no. 2.
[30] R.A.M. Buijsen, et al., FMRpolyG-Positive Inclusions in CNS and Non-CNS Organs of a Fragile X Premutation Carrier with Fragile X-Associated Tremor/ataxia Syndrome, 2014, pp. 1–5.
[31] E.R. Whittemore, Peroxide-induced cell death in primary neuronal culture 61 (4) (1995).
[32] P.K. Todd, et al., CGG repeat-associated translation mediates neurodegeneration in fragile X tremor ataxia syndrome, Neuron 78 (3) (2013) 440–455.
[33] Y. Zhang, et al., Article Secreted Monocytic miR-150 Enhances Targeted Endothelial Cell Migration, 2010, pp. 133–144.
[34] S. Das, et al., Nuclear miRNA Regulates the Mitochondrial Genome in the Heart, 2012, pp. 1596–1603.
[35] L. Sripada, D. Tomar, P. Prajapati, R. Singh, A.K. Singh, Systematic analysis of small RNAs associated with human mitochondria by deep Sequencing : detailed analysis of mitochondrial associated miRNA 7 (9) (2012).
[36] R. Zhou, et al., Mitochondria-related miR-151a-5p reduces cellular ATP production by targeting CYTB in asthenozoospermia, Sci. Rep. 5 (November) (2015) 1–10.
[37] M. Girard, N. Cagnard, S. Hanein, S. Bandiera, S. Ru, Nuclear outsourcing of RNA interference components to human mitochondria 6 (6) (2011).
[38] P.J. Magalh˜aes, A.L. Andreu, E.A. Schon, Evidence for the presence of 5S rRNA in mammalian mitochondria, Mol. Biol. Cell 9 (9) (1998) 2375–2382.
[39] A. Smirnov, N. Entelis, R.P. Martin, I. Tarassov, Biological Significance of 5S rRNA Import into Human Mitochondria : Role of Ribosomal Protein MRP-L18, 2011, pp. 1289–1305.
[40] E. Barrey, G. Saint-auret, B. Bonnamy, D. Damas, O. Boyer, Pre-microRNA and mature microRNA in human mitochondria 6 (5) (2011).
[41] L. Feng, Long Noncoding RNA 00460 (LINC00460) Promotes Glioma Progression by Negatively Regulating miR - 320a, 2019, pp. 1–8, no. October 2018.
[42] C. Li, S. Zhang, T. Qiu, Y. Wang, D.M. Ricketts, Upregulation of long non-coding RNA NNT-AS1 promotes osteosarcoma progression by inhibiting the tumor suppressive miR-320a, Cancer Biol. Ther. (2018) 1–10, vol. 00, no. 00.
[43] E. Miotto, E. Saccenti, L. Lupini, E. Callegari, M. Negrini, M. Ferracin, CEBP FOCUS Quanti Fi Cation of Circulating miRNAs by Droplet Digital PCR : Comparison of EvaGreen- and TaqMan-Based Chemistries, vol. 23, 2014 no. December.
[44] C.M. Hindson, et al., Absolute quantification by droplet digital PCR versus analog real-time PCR, Nat. Methods (september) (2013) 1–6.
[45] M.P. Rodrigues, C.J. Steer, M.A´. Mitochondria-associated, A´. Mitoplasm, A´. Purified, Mitochondrial MicroRNAs and Their Potential Role in Cell Function, 2014, pp. 123–132.
[46] L. To, T.H. E (Eds.), Identification of Mouse Liver Mitochondria-Associated miRNAs and Their Potential Biological Functions, vol. 20, 2010, pp. 1076–1078, no. 9.
[47] X. Zhang, et al., MicroRNA directly enhances mitochondrial translation during muscle differentiation, Cell 158 (3) (2014) 607–619.
[48] R. Jagannathan, et al., Translational Regulation of the Mitochondrial Genome Following Redistribution of Mitochondrial MicroRNA in the Diabetic Heart, 2015, pp. 785–802.
[49] R.F. Berman, et al., Mouse Models of the Fragile X Premutation and Fragile X-Associated Tremor/ataxia Syndrome, 2014, pp. 1–16.
[50] C. Sellier, K. Usdin, C. Pastori, V.J. Peschansky, F. Tassone, N. Charlet-Berguerand, The multiple molecular facets of fragile X-associated tremor/ataxia syndrome, J. Neurodev. Disord. 6 (1) (2014) 1–10.
[51] D.L. Shepherd, et al., “Division of exercise physiology running Title : PNPase mitochondrial microRNA import, J. Mol. Cell. Cardiol. (2017).
[52] S. Fan, et al., Mitochondrial miRNA Determines Chemoresistance by Reprogramming Metabolism and Regulating Mitochondrial Transcription, 2019, pp. 1069–1085.